



ҚАЗАҚСТАН РЕСПУБЛИКАСЫ
ТҰҢҒЫШ ПРЕЗИДЕНТІ - ЕЛБАСЫНЫҢ ҚОРЫ

«ҒЫЛЫМ ЖӘНЕ БІЛІМ – 2017»

студенттер мен жас ғалымдардың
XII Халықаралық ғылыми конференциясының
БАЯНДАМАЛАР ЖИНАҒЫ

СБОРНИК МАТЕРИАЛОВ

XII Международной научной конференции
студентов и молодых ученых
«НАУКА И ОБРАЗОВАНИЕ – 2017»

PROCEEDINGS

of the XII International Scientific Conference
for students and young scholars
«SCIENCE AND EDUCATION - 2017»



14th April 2017, Astana



**ҚАЗАҚСТАН РЕСПУБЛИКАСЫ БІЛІМ ЖӘНЕ ҒЫЛЫМ МИНИСТРЛІГІ
Л.Н. ГУМИЛЕВ АТЫНДАҒЫ ЕУРАЗИЯ ҰЛТТЫҚ УНИВЕРСИТЕТІ**

**«Ғылым және білім - 2017»
студенттер мен жас ғалымдардың
XII Халықаралық ғылыми конференциясының
БАЯНДАМАЛАР ЖИНАҒЫ**

**СБОРНИК МАТЕРИАЛОВ
XII Международной научной конференции
студентов и молодых ученых
«Наука и образование - 2017»**

**PROCEEDINGS
of the XII International Scientific Conference
for students and young scholars
«Science and education - 2017»**

2017 жыл 14 сәуір

Астана

УДК 378

ББК 74.58

Ғ 96

Ғ 96

«Ғылым және білім – 2017» студенттер мен жас ғалымдардың XII Халықаралық ғылыми конференциясы = The XII International Scientific Conference for students and young scholars «Science and education - 2017» = XII Международная научная конференция студентов и молодых ученых «Наука и образование - 2017». – Астана: <http://www.enu.kz/ru/nauka/nauka-i-obrazovanie/>, 2017. – 7466 стр. (қазақша, орысша, ағылшынша).

ISBN 978-9965-31-827-6

Жинаққа студенттердің, магистранттардың, докторанттардың және жас ғалымдардың жаратылыстану-техникалық және гуманитарлық ғылымдардың өзекті мәселелері бойынша баяндамалары енгізілген.

The proceedings are the papers of students, undergraduates, doctoral students and young researchers on topical issues of natural and technical sciences and humanities.

В сборник вошли доклады студентов, магистрантов, докторантов и молодых ученых по актуальным вопросам естественно-технических и гуманитарных наук.

УДК 378

ББК 74.58

ISBN 978-9965-31-827-6

©Л.Н. Гумилев атындағы Еуразия
ұлттық университеті, 2017

UDK 621.43.068.4

INTERACTION OF $^{6,7}\text{Li} + ^{28}\text{Si}$ AT LOW ENERGIES IN THE FRAMEWORK OF THE DOUBLE-FOLDING MODEL

Azhibekov Aidos

azhibekoaidos@mail.ru

Master of Nuclear Physics 2nd year, Physico-Technical Faculty, L.N.Gumilyov ENU, Astana
Supervisor – K.Kuterbekov

Abstract

The experimental data on elastic scattering of $^{6,7}\text{Li}$ ions on ^{28}Si nuclei in the energy range from 7.5 to 36 MeV have been analyzed in the framework of the double-folding model on the basis of BDM3Y-Paris and M3Y-Paris potentials. Analysis of the dependence of the volume integrals of the potential on the energy of the incident particle enabled us to find common energy dependencies for interactions of $^{6,7}\text{Li}$ nuclei. The energy dependencies of the total reaction cross sections obtained in this work are in good agreement with the experimental data.

1. Introduction

Nowadays, one of the most important tasks in nuclear physics is studying of elastic and inelastic scattering of cluster and exotic nuclei. Investigation of interactions of light weakly-bound cluster nuclei with other nuclei provides important information on the structure and mechanisms of nuclear reactions, in particular, the data on parameters of the scattering potential of these types of nuclei.

The analysis of the differential cross sections of elastic scattering does not give unambiguous values of macroscopic optical potentials. It is well-known that there are two types of uncertainty in the determination of nuclear potentials: discrete and continuous. This uncertainty is explained by the fact that the internal part of the potential usually feels partial waves with small values of the orbital momentum l , whose contribution to the scattering cross section is very small. Therefore, any potentials with close values of parameters in the nuclear periphery or potentials correctly predicting phases for a limited number of partial waves with a maximum contribution to the cross section have similar angular distributions of elastic scattering at low energies.

Double-folding potential (DFP) can be considered as a semi-microscopic optical potential, well describing the experimental data. This method, widely used nowadays, is attractive for its realism from the viewpoint of the theory. This model takes into account not only the density distribution of nuclear matter, but also the nucleon-nucleon potential accounting for interactions on a microscopic level and depending on the density of nucleons within the nucleus. Taking into account the theoretical justification of the model [1], we analyzed the elastic scattering $^{6,7}\text{Li}$ ions on ^{28}Si nucleus in the framework of the double-folding model.

2. Formalism

The semi-microscopic optical potentials $U(R)$ are constructed in the double-folding model using the effective nucleon-nucleon BDM3Y-Paris and M3Y-Paris interaction potentials as well as nucleon densities.

The difference between interactions is based on the dependence of the BDM3Y-Paris potential on the density of nucleons in the nucleus. The potential of interaction of two colliding nuclei can be written as:

$$U(R) = \int \int \rho_1(r_1)\rho_2(r_2)V_{NN}(R - r_1 + r_2)d^3r_1d^3r_2, \quad (1)$$

where integration is made over the volume of the projectile and the target, $V_{NN}(R - r_1 + r_2)$ is the effective nucleon-nucleon interaction (BDM3Y-Paris or M3Y-Paris), $\rho_i(r_i)$ is the distribution

of nuclear matter of the projectile and the target ($i = 1, 2$). Densities are obtained from the experimental data.

In the framework of the double-folding model, the effective nucleon-nucleon BDM3Y-Paris interaction can be written in a factorized form:

$$V_{NN}(r, \rho, E) = f(\rho)V_{NN}(r, \rho, E) \quad (2)$$

The factor of density dependence (the influence of nuclear medium) is selected in the standard form:

$$f(\rho) = C(1 + \alpha e^{-\beta\rho} + \gamma\rho) \quad (3)$$

Parameters $C=1.2521$, $\alpha=0$, $\beta=0$ and $\gamma=1.7452$ are found from the comparisons of the volume integrals after substitution of these parameters with volume integrals of the G-matrix elements, constructed in the framework of the nuclear matter theory [2].

The total optical DFM potential has not only a real part but also an imaginary part, responsible for the absorption of the incident particle in the inelastic channels.

The absorption potential was constructed in the framework of two approaches – in the Woods-Saxon form (4) and in the form, depending on the calculated real part (5):

$$W(R) = W_0(1 + \exp(R - r_w)/a_w))^{-1} \quad (4)$$

$$W(R) = N_1 U(R, \rho, E) \quad (5)$$

Where N_1 is the factor normalizing the depth of the imaginary part of the potential. Thus, the total optical DFM potential is written as:

$$U_t(R) = N_R U(R) + iW(R) \quad (6)$$

Where N_R is the factor normalizing the depth of the real part of the potential. It should be noted that $U(R)$ has two forms: BDM3Y-Paris and M3Y-Paris.

In formulas (5 – 6), $N_{R,i}$ are parameters of the potential, which are varied in order to get the best agreement with the experimental data on the differential cross sections and the total reaction cross sections.

The search for optimal parameters of the potentials was carried out by minimizing the value of χ^2 :

$$\chi^2 = \frac{1}{N_e} \sum_{i=1}^{N_3} \left[\frac{\sigma^T(\theta_i) - \sigma^e(\theta_i)}{\Delta\sigma^e(\theta_i)} \right]^2 \quad (7)$$

Where N_e is the number of experimental points in the angular distribution, σ^T and σ^e are the calculated and measured values of the differential scattering cross section at an angle θ_i , $\Delta\sigma^e$ is an uncertainty of $\sigma^e(\theta_i)$.

The double-folding potential (DFP) for BDM3Y-Paris was calculated using DFM-POT program [3] and for M3Y-Paris using the DF-POT program [4]. Differential and total reaction cross sections were calculated by the FRESCO program [5].

The matter density distributions for ${}^6,7\text{Li}$ nuclei obtained from electron scattering (Figure 1) have the following form:

$$\rho_1^{6Li}(r_1) = 0.203 \exp(-0.3306 \exp r_1^2) + (-0.0131 + 0.001378 r_1^2) \exp(-0.1584 r_1^2) \text{fm}^{-3} \quad [7], \quad (8)$$

$$\rho_1^{7Li}(r_1) = 0.1387(1 + 0.1673 r_1^2) \exp(-0.3341 r_1^2) \text{fm}^{-3} \quad (9)$$

For these configurations of densities the rms radii of ${}^6\text{Li}$ and ${}^7\text{Li}$ nuclei are equal to 2.394 fm and 2.403 fm, respectively.

As the nuclear matter density distribution for ${}^{28}\text{Si}$ nucleus in the ground state, we used the harmonic oscillator function with the standard radius of the nucleus of 3.137 fm (Fig. 1) [9]:

$$\rho_2^{28\text{Si}}(r_2) = 0.2050(1 + 0.1941r_2^2)\exp(-0.2112r_2^2)\phi\text{M}^{-3} \quad (10)$$

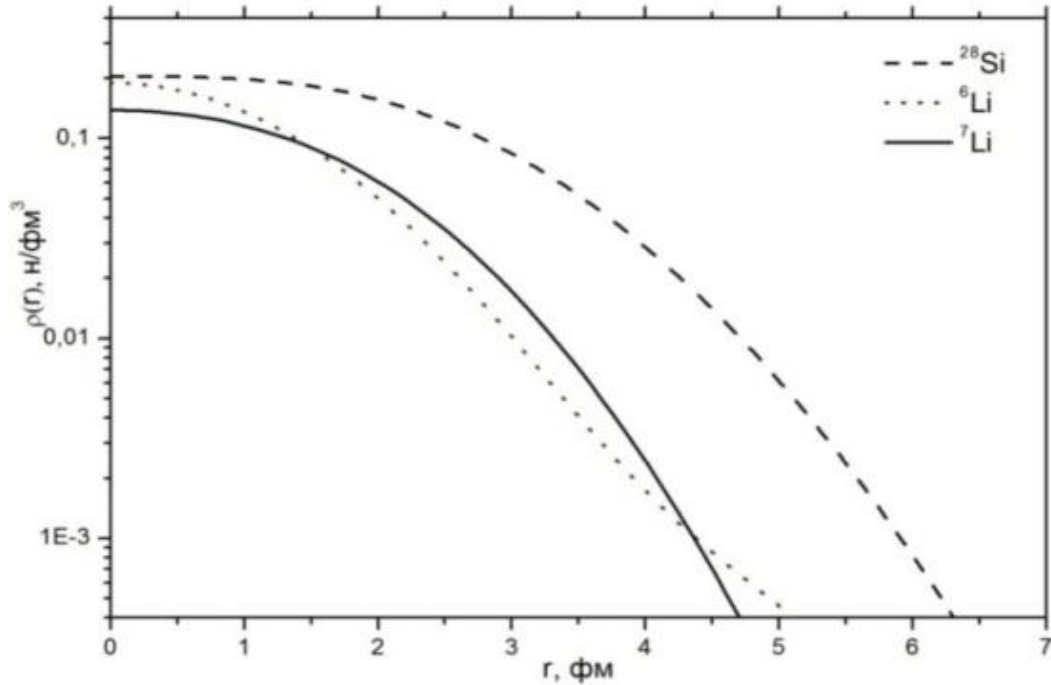


Figure 1. The matter density distribution for ${}^{6,7}\text{Li}$ and ${}^{28}\text{Si}$ nuclei.

3. Analysis of the experimental data

Tables 1, 2 and 3 present values of parameters of $U_t = N_R U(r, \rho, E) + iW^{\text{WS}}$, $U_t = N_R U(r, E) + iW^{\text{WS}}$ and $U_t = N_R U(r, \rho, E) + iN_I U(r, \rho, E)$ potentials for ${}^{6,7}\text{Li} + {}^{28}\text{Si}$ reactions.

Table 1

Parameters of $U_t = N_R U(r, \rho, E) + iW^{\text{WS}}$ potential for ${}^{6,7}\text{Li} + {}^{28}\text{Si}$ elastic scattering

$E_{\text{лаб}}$ (МэВ)	N_R	W (МэВ)	r_w (фМ)	a_w (фМ)	χ^2
${}^6\text{Li} + {}^{28}\text{Si}$					
9	0.33	27.60	1.270	0.700	0.581
13	0.49	29.40	1.170	0.690	0.292
20	0.57	8.50	1.360	0.590	1.296
25	0.72	10.60	1.364	0.517	6.596
32	0.56	27.50	1.170	0.690	2.115
${}^7\text{Li} + {}^{28}\text{Si}$					
8	0.275	10.0	1.16	0.667	0.120
8.5	0.279	10.0	1.16	0.653	0.427
9	0.289	22.55	1.10	0.668	0.114
13	0.410	30.0	1.16	0.665	0.401
16	0.560	31.16	1.20	0.643	0.255
20	0.409	15.70	1.19	0.653	5.861
26	0.60	20.481	1.20	0.660	5.871
36	0.594	24.21	1.20	0.658	15.786

Table 2

Parameters of $U_t=N_R U(r,E)+iW^{WS}$ potential for ${}^6,7\text{Li} + {}^{28}\text{Si}$ elastic scattering

$E_{\text{лаб}}$ (МэВ)	N_R	W (МэВ)	r_w (фМ)	a_w (фМ)	χ^2
${}^6\text{Li} + {}^{28}\text{Si}$					
9	0.458	24.949	1.200	0.690	0.168
13	0.490	16.170	1.200	0.690	0.608
20	0.630	8.700	1.360	0.590	3.939
25	0.756	11.519	1.350	0.550	6.401
32	0.674	27.500	1.170	0.690	2.115
${}^7\text{Li} + {}^{28}\text{Si}$					
8	0.330	10.50	1.16	0.667	0.121
8.5	0.342	11.00	1.16	0.653	0.427
9	0.337	20.00	1.10	0.668	0.124
13	0.498	31.00	1.16	0.665	0.476
16	0.680	33.45	1.20	0.643	0.264
20	0.463	14.83	1.19	0.653	5.861
26	0.686	20.89	1.20	0.660	5.871
36	0.708	24.00	1.20	0.658	15.786

Table 3

Parameters of $U_t=N_R U(r,\rho,E)+iN_I U(r,\rho,E)$ potential for ${}^6,7\text{Li} + {}^{28}\text{Si}$ elastic scattering

${}^6\text{Li} + {}^{28}\text{Si}$				
$E_{\text{лаб}}$ (МэВ)	N_R	N_I	χ^2	
9	0.319	0.418	0.39	
13	0.400	0.450	0.67	
20	0.580	0.125	17.7	
25	0.800	0.260	21.4	
32	0.550	0.550	03.1	
${}^7\text{Li} + {}^{28}\text{Si}$				
8	0.275	0.180	0.121	
8.5	0.279	0.112	0.420	
9	0.289	0.249	0.115	
13	0.400	0.465	0.410	
16	0.556	0.605	0.261	
20	0.416	0.342	6.266	
26	0.635	0.465	5.972	
36	0.591	0.513	14.182	

Figure 2 shows the energy dependence of parameters of $U_t=N_R U(r,\rho,E)+iN_I U(r,\rho,E)$ potential. It is seen that the normalizing factors N_U and N_I for the reaction of ${}^7\text{Li} + {}^{28}\text{Si}$ elastic scattering have a common behavior shown by the line. At energies ranging from 13 to 36 MeV, the values of both parameters are at the level of 0.4 – 0.635, with a decrease in energy they fall to the level of 0.112 – 0.289. For the purpose of visualization, the energy range is divided by the energy of the Coulomb barrier ($E_{c,b.}=8.69$ MeV) [6].

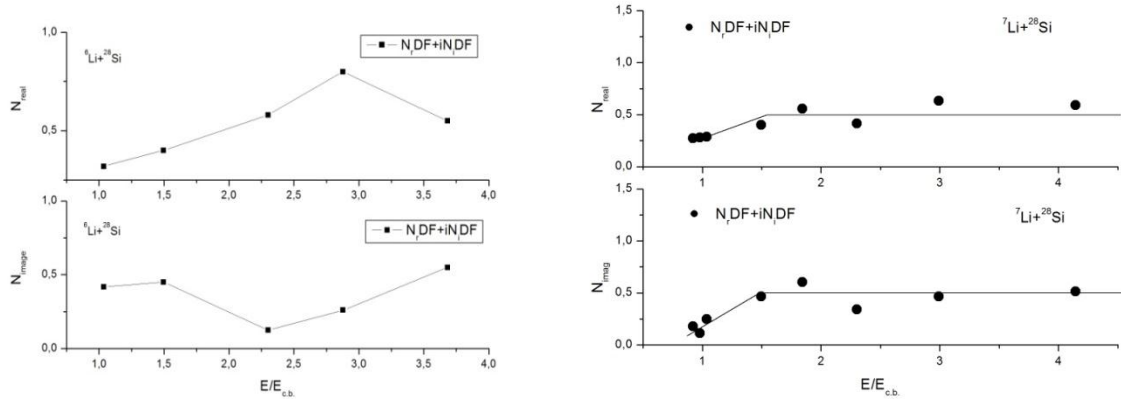


Figure 2. Energy dependence of normalizing factors N_U and N_I for ${}^6\text{Li} + {}^{28}\text{Si}$ (left) and ${}^7\text{Li} + {}^{28}\text{Si}$ (right). The solid line (right) shows the general trend in the energy dependence.

Figure 3 shows the results of a comparative analysis of angular distributions of the differential cross sections for elastic scattering of ${}^{6,7}\text{Li}$ ions on ${}^{28}\text{Si}$ nucleus at different energies using $U_t = N_R U(r, \rho, E) + iW^{WS}$, $U_t = N_R U(r, E) + iW^{WS}$ and $U_t = N_R U(r, \rho, E) + iN_I U(r, \rho, E)$ potentials. It is seen that the curves calculated in this work in terms of two approaches give a good description of the angular distributions of experimental cross sections.

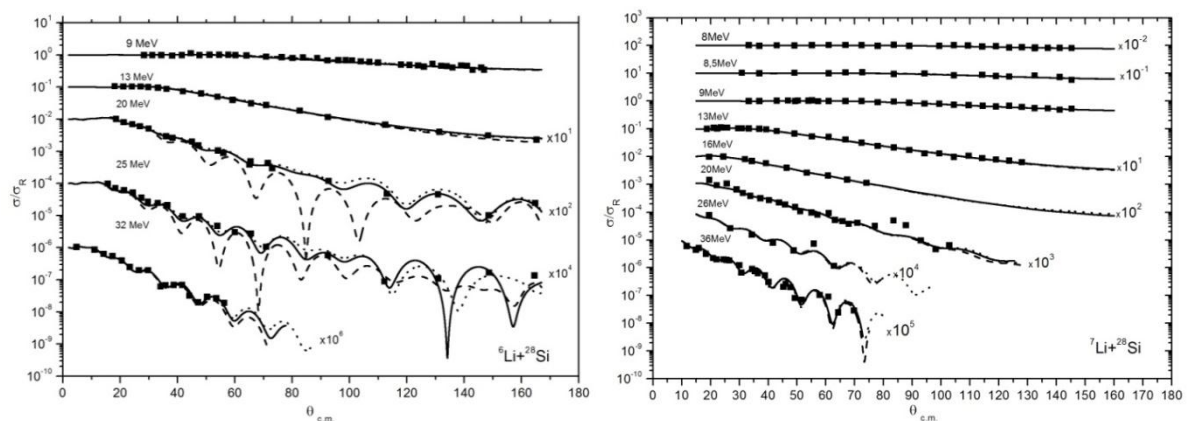


Figure 3. Angular distributions of differential cross sections for elastic scattering of ${}^6\text{Li}$ ions (left) and ${}^7\text{Li}$ ions (right) on ${}^{28}\text{Si}$ nucleus. Points are the experimental data [10 - 17]; the solid line is the result of calculations using $U_t = N_R U(r, \rho, E) + iW^{WS}$ potential; the dashed line corresponds to $U_t = N_R U(r, \rho, E) + iN_I N_R U(r, \rho, E)$ potential; the dotted line corresponds to $U_t = N_R U(r, E) + iW^{WS}$ potential.

In addition to the angular distributions of elastic scattering reactions, as a criterion of selection of optimal parameters we used the experimental values of the total reaction cross sections (TCS) [18]. We compared the results of calculations of the total reaction cross sections made using DFP and the Woods-Saxon potential for real and imagine part [19]. Figures 4 and 5 show that our calculations well describe the experimental data, which confirms the realisticity of cross sections calculated using the above approaches.

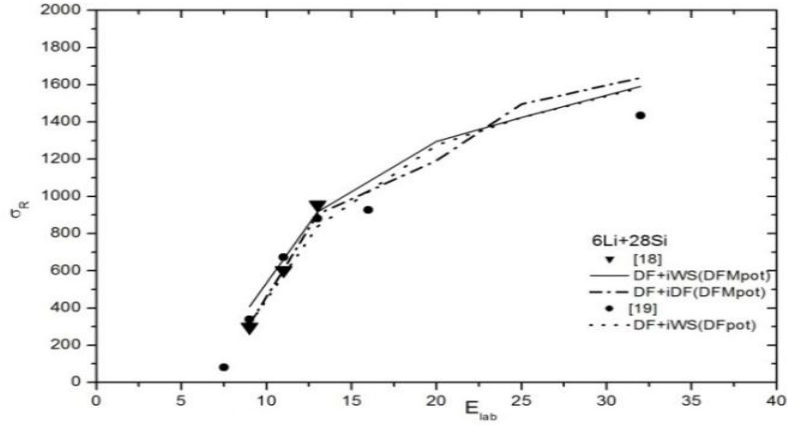


Figure 4. Energy dependence of DFP for ${}^6\text{Li} + {}^{28}\text{Si}$. ▼ denotes the data taken from [18]; ● denotes calculated TCS values taken from [19]. The solid line is the result of TCS calculations using $U_t = N_R U(r, \rho, E) + iW^{\text{WS}}$ potential; the dashed line is the result of TCS calculations using $U_t = N_R U(r, \rho, E) + iN_I U(r, \rho, E)$ potential; the dotted line corresponds to $U_t = N_R U(r, E) + iW^{\text{WS}}$ potential.

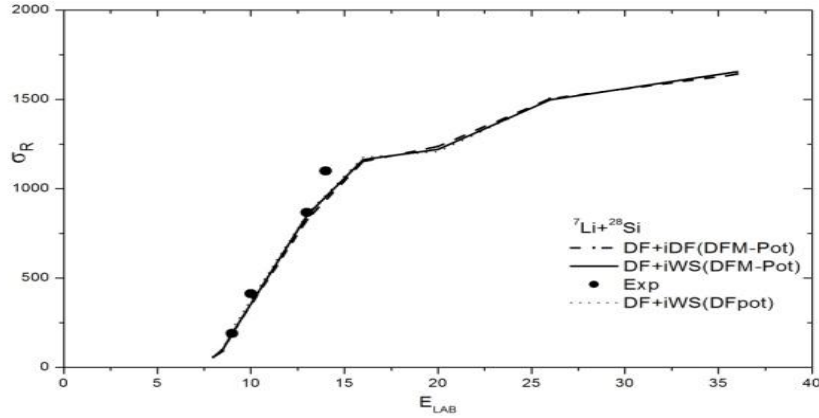


Figure 5. Energy dependence of TCS for ${}^7\text{Li} + {}^{28}\text{Si}$. Experimental data: ● – [18]. The solid line is the result of TCS calculations using $U_t = N_R U(r, \rho, E) + iW^{\text{WS}}$ potential; the dashed line is the result of TCS calculations using $U_t = N_R U(r, \rho, E) + iN_I U(r, \rho, E)$ potential; the dotted line corresponds to $U_t = N_R U(r, E) + iW^{\text{WS}}$ potential.

To obtain more information from the reaction and a more adequate description of the data, it is necessary to introduce additional integral characteristics of the potential: volume integrals of the potential and the root mean square radius of the potential. The volume integral of the nuclear potential J is a key value in determining a realistic interaction potential.

Since the selection by χ^2 does not give an unambiguous choice of parameters of the potential, as an additional criterion for selection of optimal potential parameters, we used the values of the volume integrals of the real and imaginary parts.

The volume integrals of the real and imaginary parts are calculated as follows:

$$J_V = \frac{4\pi}{A_t A_p} \int N_R V^F(r, \rho, E) r^2 dr. \quad (10)$$

$$J_W = \frac{4\pi}{A_t A_p} \int N_I V^F(r, \rho, E) r^2 dr, \quad (11)$$

$$J_W = \frac{4\pi}{A_t A_p} \int W(r) r^2 dr, \quad (12)$$

where $A_{p,t}$ are mass numbers of the projectile and target nucleus, $V^F(r,\rho,E)$ and $W(r)$ are the real and the imaginary parts of the potential of nuclear interaction.

The energy dependences of the volume integrals for elastic scattering reactions of exotic and cluster nuclei show a common trend for the real and imaginary parts of the volume integrals [20,21].

Figure 6 shows the energy dependences of the volume integrals of the real and imaginary parts of the potential for ${}^6\text{Li} + {}^{28}\text{Si}$ elastic scattering. A symmetrical pattern is observed: the real part increases with increasing energy, whereas the imaginary part decreases. The figure shows that two different forms of potentials have the same trend in the behavior of volume integrals of the real and imaginary parts of the potential with an energy increase.

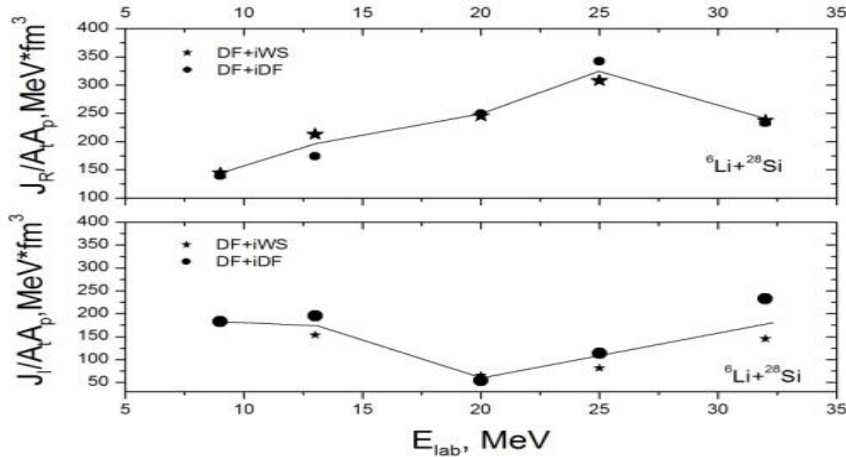


Figure 6. Energy dependences of the volume integrals of the real (top) and imaginary (bottom) parts of the potential for ${}^6,7\text{Li} + {}^{28}\text{Si}$ elastic scattering. Stars denote $V^F + iW^{WS}$, $\bullet -V^F + iV^F$. The solid line is a general trend in the energy dependence.

Figure 7 shows the energy dependences of the volume integrals of the real and imaginary parts of the potential for ${}^7\text{Li} + {}^{28}\text{Si}$ elastic scattering. It is seen that they have the same dependence on energy (the straight line). At energies of 8-16 MeV an increase in the volume integrals of both real and imaginary parts is observed. In the range of 16 - 21 MeV there is a slight decrease in the values of the integrals of both parts. For the purpose of visualization, the energy scale is divided by the energy of the barrier ($E_{c.b.} = 8.69$ MeV).

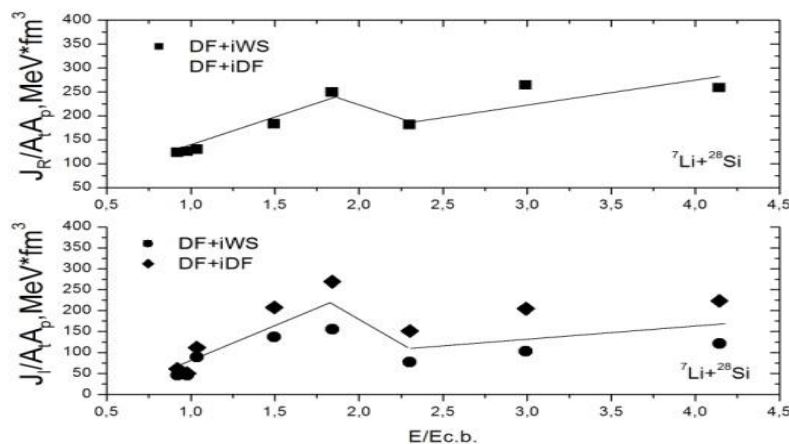


Figure 7. Energy dependences of the volume integrals of the real (top) and imaginary (bottom) parts of the potential for ${}^6,7\text{Li} + {}^{28}\text{Si}$ elastic scattering correspond to $V^F + iW^{WS} -$ to $V^F + iV^F$. The solid line shows a general trend in the energy dependence.

In terms of understanding the mechanisms of interactions it is interesting to consider the rms radii of the potentials in the framework of the double-folding model. The BDM3Y potentials for ${}^{6,7}\text{Li} + {}^{28}\text{Si}$ elastic scattering have the radii equal to 4.220 and 4.232 fm, respectively. The double-folding M3Y potentials for elastic scattering ${}^{6,7}\text{Li} + {}^{28}\text{Si}$ have the radii 4.492 and 4.454 fm, respectively.

4. Conclusion

The experimental data on elastic scattering of ${}^{6,7}\text{Li}$ ions on ${}^{28}\text{Si}$ nucleus in the energy range from 7.5 to 36 MeV were analyzed in the framework of the optical model using various forms of potentials. All the approaches used in the work enabled us to obtain a good description of the experimental data on the differential and total reaction cross sections for the ${}^{6,7}\text{Li} + {}^{28}\text{Si}$ interaction. The paper analyzes the dependence of the volume integrals on the energy of the incident particle. The parameters of the potential and the energy dependencies obtained in this work enable us to make a conclusion about realism of our potential parameters and mean square radii.

References

1. G.R. Satchler and W. G. Love // Review Section of Physics Letters 55, No.3 (1979) P.183-254.
2. Madsen V.A., Brown V.R. // Phys. Rev., 1975, V. C12, P. 1205.
3. J. Cook // Computer Physics Communications 25 (1982) 125-139
4. Lukyanov K V et al //Bull.Rus.Acad.Sci.Phys. 72 382, 2008.
5. I. J. Thompson //Computer Physics Reports, 7 (1988) pp 167 – 212
6. K.H. Bray, M. Jain // Nucl. Phys. A 189 (1972) 35.
7. M. El-Azab Farid; M.A. Hassanain // Nuclear Physics A Volume 697 issue 1-2
8. O.M. Knyazkov, E.F. Hefter, Z. // Phys. A 301 (1981) 227.
9. M. Sinha et. al. // EPJ Web of Conferences, 17 (2011) 03004.
10. M. HUGI et al. // Nuclear Physics, A368 (1981) 173-188.
11. N. Anantaraman, H.W. Fulbright, P.M. Stwertka // Phys. Rev., C22 (1980) 503.
12. A. Nadasen et al. //Physical Review, C39 (1989) 536-545.
13. A. Pakou et al.// Physical Review, C69 (2004) 054602
14. Mandira Sinha et al. // EPJ Web of Conferences, 17 (2011) 03004
15. K.Bethge et al.// Nuclear Physics, A123 (1969) 521-530
16. P. Schumacher et al.// Nuclear Physics, A212 (1973) 573-599
17. A. Pakou et al. // Nuclear Physics A 784 (2007) 13–24
18. K.A.Kuterbekov et al.// Phys.Atomic Nuclei 77, 581 (2014); Yad.Fiz. 77, 615 (2014)
19. Y. Kucuk et al. // Nuclear Physics, A 927 (2014) 195–208
20. M. Y. H. Farag et al.// PHYSICAL REVIEW C 88, 064602 (2013)

UDC 523.98; 551.521:523; 551.590.21

THE COSMIC RAY DETECTOR CARPET/ASTANA

Sakhabayeva Saira

m.saira1405@gmail.com

Master of Nuclear Physics 2nd year Physico-Technical Faculty L.N.Gumilyov ENU, Astana
Scientific supervisor – Sh.Giniyatova

In 2016 at physico-technical faculty of the L.N. Gumilev Eurasian national University (Astana, Kazakhstan 51°10'48" n, 71°26'45" e, altitude 358m, the rigidity of the geomagnetic circumcison $R_c \sim 2.5$ GeV), the cosmic ray detector CARPET was commissioned. The detector is designed and created in the Physical Institute of the P. N. Lebedev Academy of Sciences in the framework of the agreement on international cooperation between the Lebedev physical Institute